Polymer Bulletin 17, 141–148 (1987)

Polymer Bulletin

Solid state and solution features of amylose and amylosic fragments

Serge Perez* and Caroll Vergelati

Centre de Recherches sur les Macromolécules Végétales, C.N.R.S., BP68,
F-38402 Saint Martin d'Hères, France

ABSTRACT

An understanding of the molecular changes occurring during polymorphic transformations of amylose is sought through the use of energy calculations. Four stable families of low energy conformers are found; three of these correspond to conformations observed in linear and cyclic maltodextrins in the crystalline state. Upon change of solvent, significant variations have been shown to occur in the relative abundance of amylose conformers. This, in turn, influences properties such as chain extension. The relevance of the stable conformers with respect to helical structures of amylose is analyzed. Whereas one of the conformers would generate a V type shallow helix, another one would give rise to a 6 fold left-handed strand having a 3.6 A advance per residue. This would generate a double helical stranded structure.

INTRODUCTION

In order to correlate the chemical structure of a biopolymer with its biological and physical properties, accurate representation of the conformational energy space of oligomeric units has to be sought (1). In the case of a homopolymer, the basic assumptions for computing the conformational energy surface of a dimeric unit relies upon the fact that, quite often, only the non-bonded interactions between atoms belonging to to nearest neighbor residues are important. In doing so two more hypothesis are implied: the free-space approximation, i.e. the solvent and possible very long range interactions are neglected. In the field of conformational analysis, the calculated stable conformers are usually compared to the results gathered from solid state investigations on model compounds in the crystalline state. In the case of amylose, which has received more attention than any other polysaccharide, accumulation of crystalline data on several linear and cyclic maltodextrins has shown that several stable conformations can be found. They provide an accurate set of experimental data which should, ideally, be reproduced by energy calculations. The present work analyzes the suitability of using "empirical" potential energy functions in the prediction of the occurrence of the low energy conformers of maltose. This work is also aimed at understanding the molecular changes which occur during polymorphic transformations of amylose.

* To whom offprint requests should be sent

CONFORMATIONAL ANALYSIS

The dimeric fragment of amylose: maltose has been used as the starting unit on which conformational analysis was performed. The labelling of the atoms, shown in Fig. 1, proceeds from the non reducing end (unprimed atoms) to the reducing end (primed atoms). The sign of the torsional angles is given according to the rules of the IUPAC-IUP Commission on Biochemical Nomenclature .

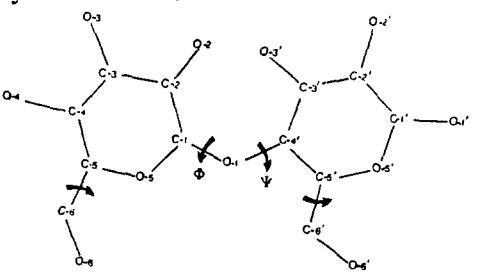

Schematic representation of the maltose molecule, along with the torsional angles of interest.

The potential energy was calculated by including the partitioned contributions arising from the van der Waals, torsional and hydrogen bond contributions (2). The van der Waals interactions were evaluated by using the 6-12 potential functions with the parameters proposed by Scott and Scheraga (3). A three fold sinusoidal potential was used for rotation about the glycosidic bond O-1 - C-4' with a barrier of 1.0 kcal/mol. In order to represent the intramolecular mechanism responsible for the exo-anomeric effect, the following function (4) was used for rotation about the glycosidic bond C-1 -O-1 :

$$EAE(\Phi) = -1.33(1-\cos\Phi)-0.62(1-\cos 2\Phi)+0.35(1-\cos 3\Phi)-2.92\sin\Phi-0.74\sin 2\Phi$$

A sinusoidal three-fold eclipsed rotational barrier of 1 kcal/mol is also used. Hydrogen bond energies were computed by an empirical expression :

$VHB = 33.14\ (R - 2.55)\ (R - 3.05)$, where R is the distance between oxygen atoms which should lie between 2.55 and 3.05 A. This expression is derived from the results of a survey on 210 hydrogen bonds as occuring in crystalline carbohydrates. Fig. 2 is the histogram of the distribution of O...O distances found. The stabilizing energy is given a maximum amplitude of -2.0 kcal/mol. The factor 33.14 is computed in order for the energy to be expressed in kcal/mol. No electrostatic interaction was taken into account. The energy maps were computed as a function of Φ and Ψ at intervals of 5°. With respect to the relative energy minimum, iso-energy contours were drawn by interpolation of 1 kcal/mol. The 12 kcal/mol contour was selected as the outer limit.

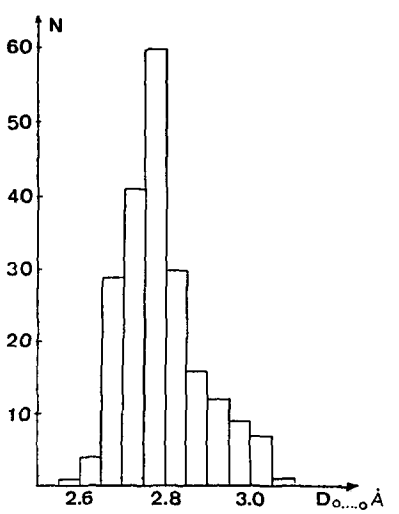

Fig. 2. Histogram of the distribution of O...O distances, involved in the hydrogen bonding formations observed in crystal structures of carbohydrates.

The geometry of the α-D-glucose residues has been shown to vary to some extend (5); for example, despite a relative constancy of the C-4...C-1 distances, a wide range of variations from 4.052 to 4.575 A were detected for O-4...O-1. In view of these findings, the estimations of the energy magnitude were performed using a geometry of the disaccharide derived from the corresponding family as found in the solid state. As for the orientation of the primary hydroxyl group, it has already been shown (6) that it has no influence on the stable conformations about the glycosidic junction between two α (1→4) linked glucose residues. Therefore, one among the preferred conformations (gauche-gauche) was selected and left invariant. The molecular drawings were obtained with the aid of the PITMOS (7) program.

CALCULATED VERSUS SOLID-STATE CONFORMATIONS OF AMYLOSIC FRAGMENTS.

The iso-energy maps were calculated, using three different starting geometries for the maltose residue, respectively taken from the structure of β-maltose (8), phenyl-α-maltoside (9) and the non-reducing disaccharide of the maltotriose molecule (10). In all cases, computations were performed with and without the contribution of intramolecular hydrogen bonds. A typical iso-energy contour map is shown on Fig. 3. It corresponds to a situation where the hydrogen bond contribution has been taken into account (Fig. 3). Two distinct regions of the (Φ, Ψ) space define the low energy domains. The low energy area spanning from Ψ =-80° to Ψ =-190° contains all the crystallographically observed minima.

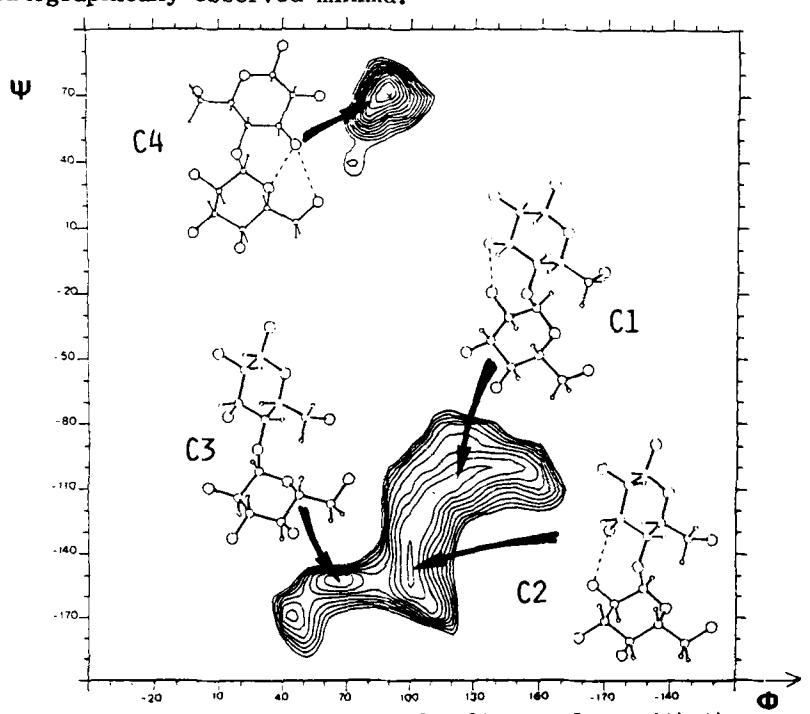

Fig. 3. Iso-energy contour map of maltose, along with the representation of the four stable conformers.

Three stable conformers, namely C1, C2 and C3 are found in this zone. The second low energy domain is centered around Ψ =70°; it corresponds to conformation of maltose molecule (C4) where Ψ has been rotated by approximately 180° from the previous conformations. It is noticeable that the 4 kcal/mol energy contour delimits a zone that encompasses more than 80% of the available surface. The introduction of energy contribution arising from intramolecular hydrogen bonding results in a significant alteration of this low energy region. The intramolecular energies of maltose residue corresponding to these stable conformations are listed in Table 1, along with the solid state conformations observed in crystalline linear maltodextrins. Whereas conformers C1, C2 and C3 correspond closely to conformations found in the solid state, conformer C4 has not yet be found. As for the three stable conformations C1, C2 and C3 it is clear that they correspond to molecular arrangements where the magnitude of the non-bonded interactions is quite similar. (In the case of conformer C4, a value larger by about 3 kcal/mol than the one obtained for the other conformers is found for the non-bonded interactions). This is also true for the energy associated with the torsional potential about the glycosidic bonds. Obviously, the main differenciating interaction appears to be the establishment of an intramolecular hydrogen bond between O-2 and O-3' of contiguous residues. Conformer C3 is the only one to occur without exhibiting such a stabilizing feature. Examination of the crystal structures corresponding to the C3 case, shows that this type of conformation is found when intramolecular hydrogen bonds are not possible, either because of the saturation of hydrogen bond possibilities (case of methyl-α-maltotrioside $4H_2O$ (10)) or because of apolar substituents (case of β-maltose octaacetate (11)).

Table 1

Intramolecular Energy (Kcal/mol) of Maltose Residue Associated with the Four Stable Conformers (A) along with their Percentage of Occurrence in Different Solvents (B).

A	C 1	C 2	C 3	C 4
Φ ,Ψ (°)	110 , -115	100 , -135	80 , -150	90 , 70
Enb	-4.04	-4.16	-4.18	-1.30
Etors	-4.12	-4.36	-4.41	-4.89
Ehb	-1.95	-1.90	none	-3.76
	O-2...O-3'	O-2...O-3'		O-5...O-3'
				O-6...O-3'
Enb+Etors	-8.16	-8.52	-8.59	-6.19
Enb+Etors+Ehb	-10.11	-10.42	-8.59	-9.95
Solid State Stable Conformations (Φ , Ψ)°	116.1, -118.0 121.7, -107.7 110.0, -108.9 105.0, -117.0	110.0, -140.0 105.0, -135.0 105.0, -135.0 105.0, -135.0	80.0, -155.0 72.0, -154.0 84.0, -154.8 82.2, -148.9 82.8, -151.8	
H-1...H-4'(A)	2.04	2.14	2.52	3.57
B				
p-dioxane (%)	20.3	53.3	17.7	8.7
ethanol (%)	20.7	42.0	22.1	15.2
DMSO (%)	21.8	40.1	22.8	15.3
water (%)	17.5	25.7	26.3	30.5

Φ = O-5 - C-1 - O-1 - C-4' ; Ψ = C-1 - O-1 - C-4' - C-5'

MODELING OF SOLUTION BEHAVIOR

The occurrence of four families of stable conformations for the maltose disaccharide is corroborated by independent calculations, based upon either rigorous semi-empirical methods (12), molecular mechanics calculations (2) and other force field methods (13). From the latter case, the four derived conformers were further submitted to PCILO refinement in order to assign partial charges, prior investigating the conformational equilibria in different solvents (14). The pertinent data giving the variations in the distributions of conformers C1, C2, C3 and C4 on going from non polar to polar solvents are listed in Table 1.

In principle, the disaccharide energy surface represents the starting point for an analysis of the solution behavior of polysaccharides. Obviously, it conveys also pertinent information to be used in modeling experimental observables such as : coupling constants (15), nuclear Overhauser effects (12), spin lattice relaxation times, as well as optical rotation at a single wavelength. All these are sensitive to conformational changes about the glycosidic linkage; they reflect a thermodynamically averaged conformation. In what follows, some of these observables will be modeled based on the concept of the existence of a limited number of stable conformers, for which the percentage of occurrence can be readily computed. On the (Φ,Ψ) map, four starting zones, respectively centered around conformers C1, C2, C3 and C4 were considered; each zone had a surface of about $200^{\circ 2}$. In a given solvent the probability of occurrence of each zone was taken to be equal to that of the corresponding conformer; then, within a given zone, the occurrence of any conformation was considered to be equiprobable.

The average value of the linkage rotation is based on values for individual conformers, determined from the expression given by Rees (16) : $\Lambda = -105 - 120\ (\sin \Phi^H + \sin \Psi^H)$ where Φ^H and Ψ^H are the glycosidic torsion angles referred to the hydrogen atoms. Our calculated value for $\langle \Lambda \rangle$ in water is -17.8° , from which an α_D value of 171° can be derived for amylose. This is to be compared to the measured value of 195° 5° reported for amylose just before gelation takes place (17).

Chain extension, as well as the conformational freedom of a polymer can be outlined by the plot of the characteristic ratio $C(\underline{n})$ as a function of the degree of polymerization $\underline{n}$ (18,19). Within the framework describe above, chain samples with $\underline{n}$=5000 were generated for each solvent considered in this study. The characteristic $C(\underline{n})$ was evaluated and its variation as a function of $\underline{n}$ was checked for asymptotic behavior. The results are reported in Table 2. The fact that C_∞ in water, is obtained for a $\underline{n}$ value in the vicinity of 70 as

Table 2

	vacuum	dioxan	DMSO	water
C_∞	1.7	1.6	2.3	4.0
$\underline{n}$	60	50	50	70

compared to values of 50 in other solvents, indicates a greater extension of the amylosic chain in this particular solvent. In agreement,

the value of C_∞ is larger in water than in vacuum and the values for other solvents lie in between, being roughly a function of the dielectric constant of the media.

As far as the calculated conformations about the angle (C-1-O-1) bond) are concerned, the present results may be extended to the general behaviour observed for the type of linkages in crystalline carbohydrates. A study of the dispersion of the angles in all reported α-linked D glucose residues (20) indicated that, despite the wide variety of linkage types, the variation of was indeed restricted, and a bimodal distribution was observed (Fig. 4). One of the node is found to be centered around $\Phi=80°$ ranging from 60° to 85°, and corresponds to structures that do not exhibit any intramolecular hydrogen bonding. Clearly, such a mean conformation corresponds to cases where only non-bonded interactions and the exo-anomeric effect are preponderant. Decomposition of the calculated energy into its main contributors (Table 1) shows that the non-bonded interactions between conformers does not differ. Considerations of the conventional functions used to express the influence of the exo-anomeric effect (21) would predict a stable minimum at $\Phi = 60°$. In our present scheme, the stable conformation about is found to be shifted by about 20° away from this perfectly stagered position, and indeed reflects, in a satisfactory manner, the observed conformations about C-1 -O-1 bond (Fig. 4). The other node as observed on the histogram is found to be centered at $\Phi = 110°$ (ranging from 100° to 120°) and is associated with oligosaccharides having a hydrogen bond between contiguous residues. Clearly for these latter values the stabilizing influence of the exo-anomeric effect is overriden by the formation of an intramolecular hydrogen bond.

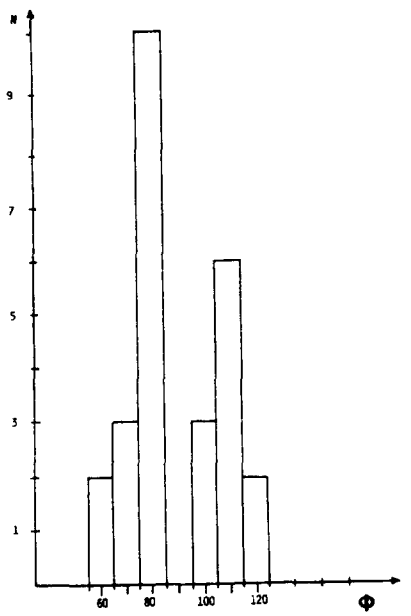

Fig. 4. Histogram of the distribution of Φ torsion angles (O-5 - C-1 - O-1 - C-x') in α-linked carbohydrates.

HELICAL PROPAGATION OF AMYLOSIC BACKBONE.

Helical arrangements are customarily described in terms of sets of helical parameters (n, h); n being the number of residues per turn of the helix, and h being the translation per residue along the helix axis. This set of parameters can be conveniently derived from the knowledge of the glycosidic torsional angles (Φ, Ψ) assuming that the other parameters remain constant. The sets of helical parameters (n, h)

based on the three stable conformers C1, C2, and C3 were evaluated. The corresponding regular helical propagation of the amylosic backbone are shown on Fig 5. Helical propagation based on conformer C3 would result in an extended chain, as shown by the magnitude of the advance per monomer h, which is almost 85% of the maximum extension. A calculated value of h = 3.6 A is indeed very close to the ones found experimentally for native A and B amyloses (22). The associated value of n = -5 indicates that the amylosic chain would display a left-handed chirality.

Incidently, small deviations away from these Φ , Ψ values would yield a left handed six fold helix from which a double helical stranded structure can be generated (23). A drastic collapse of the amylosic chain is obtained when conformer C1 is considered as defining the repeating unit. This collapse is characterized by small values of the advance per monomer h (typically around 0.5) and by values of n about -7. This again generates a left handed shallow helix which closely corresponds to the macromolecular conformation found for all the structures of amylose V or in cycloamyloses. A third type of left handed helix can be generated from conformer C2. There is a somewhat less drastic collapse of the backbone (h = 2.5 A), the helical parameter n being centered around -6.0. Such a conformation has not been reported yet for amylose polymorphs, although it is preponderant in maltoheptaose bound to phosphorylase (24).

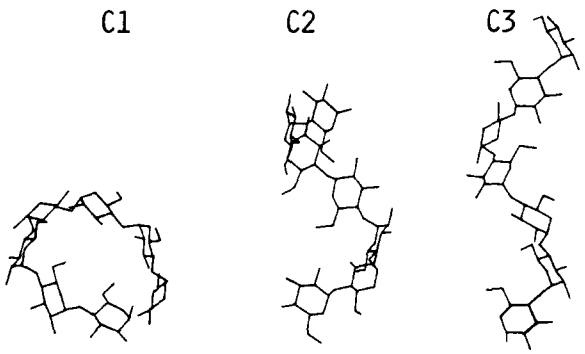

Fig. 5. Molecular drawings of three distinct maltoheptaose molecules as derived from C1, C2, C3 parent disaccharides.

CONCLUSIONS

The present work establishes that :

- the set of potential functions used in the "empirical" calculation is adequate and leads to the conclusion that four stable low energy conformers are found.

-the equilibrium between these conformational states undergoes drastic variations upon changes of the solvent. In non-polar solvents, a high proportion of the molecule exists in the conformations in which the inter residue hydrogen bond O-2...O-3' is possible. In aqueous solution, the occurrence of such stabilizing feature is no longer preponderant; this is supported by the agreement between observed and calculated optical rotation for amylose just prior to gelation.

-modeling of the polysaccharide chain in solution indicates a greater extension of the amylosic chain in water than in less polar solvents. Therefore, in going from an extended shape taken by the macromolecule in water, to a collapsed shape in less polar solvents, the chain undergoes a hydrophobic folding.

-three of the four calculated low energy minima correspond to situations observed for linear and/or cyclic maltodextrins in the solid

state. Furthermore, these conformations are shown to be precursors of a variety of left-handed helical structures. One is found to correspond closely to the amylose V type of structure, whereas another would be compatible with a left-handed double stranded helix. Another stable conformation does not correspond to any of the reported amylose polymorph, although it is preponderant in maltoheptaose bound to phosphorylase.

These findings establish that understanding of the polymorphic transformations of amylose may be reached through potential energy calculation. The present data leads to a static description only; the use of more sophisticated approaches such as molecular dynamics should lead to further insights, particularly into the pathways to interconversion between polymorphs.

REFERENCES

1. D.A. Brant, Quaterly Reviews of Biophysics, 9, 527 (1976)
2. I. Tvaroska & S. Pérez, Carbohydr. Res., 149, 389 (1986)
3. R.A. Scott & H.A. Scheraga, J. Chem. Phys., 42, 2209 (1965)
4. I. Tvaroska, Carbohydr. Res., 125, 155 (1984)
5. A.D. French & V.G. Murphy, Polymer, 18, 489 (1977)
6. S. Pérez, M. Roux, J.F. Revol & R.H. Marchessault, J. Mol. Biol., 129, 113, (1979)
7. S. Pérez & R.P. Scaringe, J. Appl. Crystallogr., 19, 65 (1986)
8. M.E. Gress & G.A. Jeffrey, Acta Crystallogr., B33, 2490 (1977)
9. I. Tanaka, N. Tanaka, T. Ashida & M. Kakudo, Acta Crystallogr., B32, 155 (1976)
10. W. Pangborn, D. Langs & S. Pérez, Int. J. Biol. Macromol., 7, 363 (1985)
11. F. Brisse, R.H. Marchessault, S. Pérez & P. Zugenmaier, J. Am. Chem. Soc., 104, 7470 (1982)
12. A.S. Shashkov, G.M. Lipkind & N.Y. Kochetkov, Carbohydr. Res., 147, 175 (1986)
13. S. Melberg & K. Rasmussen, Carbohydr. Res., 69, 27 (1979)
14. I. Tvaroska, Biopolymers, 21, 1887, (1982)
15. S. Pérez, F. Taravel & C. Vergelati, Nouv. J. Chimie, 9, 561 (1985)
16. D.A. Rees, J. Chem. Soc. B., 877 (1970)
17. D.A. Rees, Pure & Appl. Chem., 53, 1 (1981)
18. R.C. Jordan, D.A. Brant & A. Cesaro, Biopolymers, 17, 2617 (1978)
19. D. Gagnaire, S. Pérez & V. Tran, Carbohydr. Polym., 2, 171, (1982)
20. F. Longchambon, Thèse de Doctorat, Université de Paris-Nord, France (1983)
21. A. Sarko & P. Zugenmaier, "Fiber Diffraction Methods", (Eds. A.D. French & K.C. Gardner) ACS Symposium Series, 141, American Chemical Society, Washington, U.S.A. (1980)
22. R.U. Lemieux, K. Bock, L.T.J. Delbaere, S. Koto & V.S. Rao, Can. J. Chem., 58, 631, (1980)
23. A. Imberty, H. Chanzy, S. Pérez, A. Buléon & V. Tran (in preparation)
24. E. Goldsmith, S. Sprang & R. Flatterick, J. Mol. Biol., 156, 411 (1982)

Accepted January 15, 1987 C